HARD X-RAY SYNCHROTRON RADIATION MEASUREMENTS AT THE APS WITH VIBRATING WIRE MONITORS*

G. Decker[1], R. Dejus[1], S.G. Arutunian[2], M.R. Mailian[2], I.E. Vasiniuk[2]
[1] Argonne National Laboratory, Argonne, IL 60439
[2] Yerevan Physics Institute, Alikhanian Br. Str. 2, 375036, Armenia

Abstract

A 5-wire vibrating wire monitor (VWM005) was developed and tested at the Advanced Photon Source (APS). The sensor was mounted on the outboard side of a bending-magnet synchrotron radiation terminating flange in sector 37 of the APS storage ring. The parallel wires were separated vertically by 0.5 mm; however, due to the possibility of rotation about a horizontal axis, the effective distance between the wires was reduced by a significant factor. To increase the response speed, the sensor was installed in air, resulting in a step response time of less than one second. Due to the extreme sensitivity of the detector, the very hard x-ray component of synchrotron radiation was successfully measured after its passage through the terminating flange.

BACKGROUND

At the APS, insertion device photon beam position monitoring is integrated into DC orbit correction algorithms, providing submicroradian levels of pointing stability over periods greater than 24 hours. Existing photon beam position monitors (BPMs) make use of ultraviolet (UV) and soft x-ray photoemission from metallized diamond blades arranged in sets of four and positioned edge-on at the periphery of the photon beam. These monitors suffer from a number of insertion device gap-dependent systematic errors associated with unavoidable soft background radiation. This radiation is associated with strong steering correctors located immediately upstream and downstream from the undulator source; they are part of the so-called Decker distortion scheme for reducing stray radiation overall [1].

In an effort to further improve upon photon beam position monitoring, an effort was initiated in 2005 to develop a BPM that is completely insensitive to the UV and soft x-ray components of undulator beams. One active area of research is the development of PIN diodes arranged to sense copper x-ray fluorescence in the backward direction [2-4]. The present work is the culmination of a number of informal meetings that took place at DIPAC 2005, and is in fact a hybrid of Arutunian et al.'s vibrating wire monitor (VWM) concept [5] and Scheidt's work with very hard x-rays at ESRF [6].

First experiments with the VWM at the APS were conducted in vacuum with an undulator beam in early 2007 [7] using the same facility where the PIN diode measurements were made. The main conclusions from that work were that the VWM is sensitive to extremely low levels of x-ray flux, but the detector's time response is quite slow since the primary means of achieving thermal equilibrium in vacuum is through radiation. Nevertheless, the measurments and subsequent analysis have provided an interesting quantitative validation of the theory of undulator radiation. Shown in Fig. 1 are data collected for the two-wire detector installed in vacuum at APS beamline 19-ID during a vertical angle scan of the undulator source, which was a standard APS undulator A operating at a large gap of 60 mm. The principle for extracting temperature changes from individual wire acoustic resonance frequencies is described in reference [7] and in detail in reference [8], which also describes the operating principle of the device.

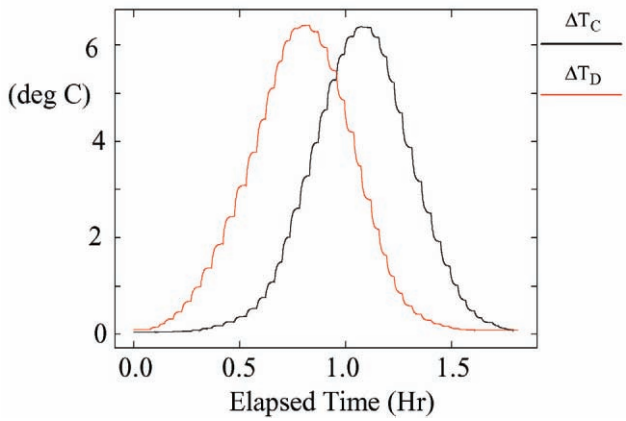

Figure 1: VWM data from undulator radiation during a vertical angle scan

The vertical angle was scanned in 5-microradian steps, pausing about three minutes after each change to reach equilibrium. As described in detail in reference [7], data analysis for this scan involved breaking the data set into 43 pieces, performing an exponential fit to each segment to extract an asymptotic temperature, executing an elaborate procedure to remove thermal drift with a linear drift model (0.01 degrees C / hour), and finally a performing normalization to stored beam current. The resulting profiles were seen to be very well approximated by Gaussians.

That the profile of an undulator beam should so closely match a Gaussian was somewhat surprising, given the known rather exotic profiles for individual undulator harmonics. To investigate this, the x-ray power density emitted from a standard APS undulator A with 60-mm gap (K = 0.023) was calculated after passing through 7 mm of beryllium [9]. This calculation included the particle beam dimensions, using a natural emittance of 2.5 nm-rad and 1% horizontal / vertical coupling. Shown

*Work supported by U.S. Department of Energy, Office of Science, Office of Basic Energy Sciences, under Contract No. DE-AC02-06CH11357.

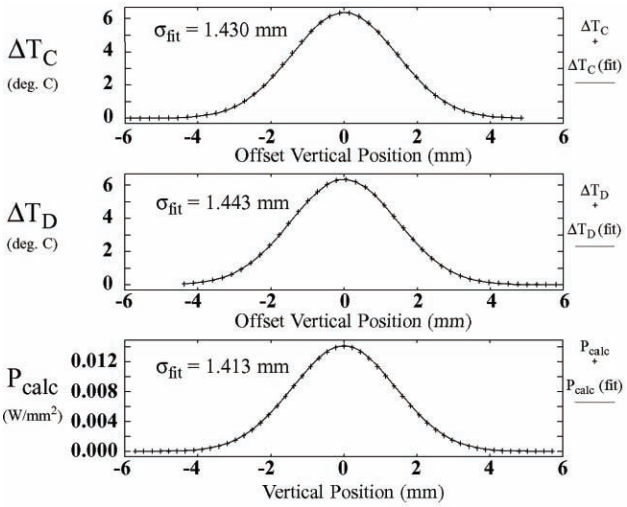

Figure 2: Comparison of experiment and theory: vertical profile of undulator radiation for APS undulator A, K = 0.023. Top and center: VWM data, shifted along the horizontal axis for the two wires C and D, with Gaussian fits. Bottom: calculated power density with Gaussian fit.

Fig. 2 is a comparison between the processed VMW profiles and the calculated power density.

As can be seen, the agreement is remarkable, to within about 2% in rms beam size. Nevertheless, the theoretical profile is non-Gaussian in detail. Shown in Fig. 3 are the residuals to the respective fits.

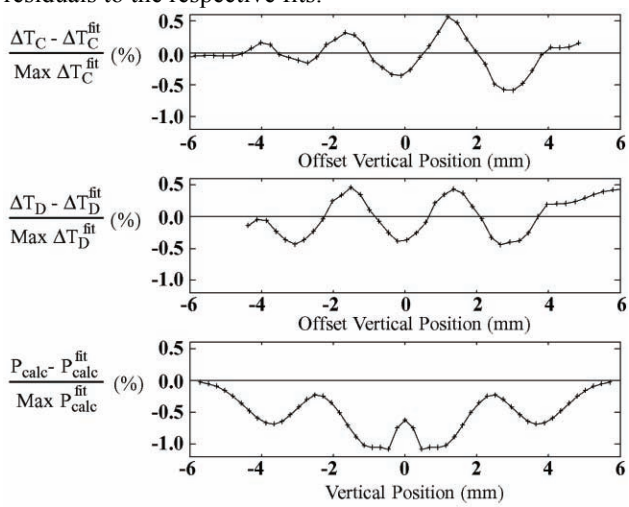

Figure 3: Undulator radiation Gaussian fit residuals.

The first thing to notice here is that the theoretical residual is unipolar. Since there is no ambiguity with regard to the zero-power baseline, the Gaussian fit was constrained to have zero baseline. This is clearly not the case for the experimental data, where unknown components of thermal drift introduce uncertainties as to the value of the baseline, which was used as a variable in the fit, along with centroid position and sigma. The scale of the residuals, and to some extent the shape, show good agreement. It is important to keep in mind that while the VWM provides a reliable measure of power deposited, in this case we are dealing with hard x-rays, and there clearly is a wavelength-dependent aspect to x-ray absorption in the wires. For the calculation, the total power density is computed, irrespective of material properties other than the 7-mm beryllium absorber placed in the path of the x-ray beam. An additional consideration, specifically with regard to the sigma values, is that the horizontal axis for the experimental data is wholly determined by the rf BPM calibrations, which are probably not accurate at the level of 2 to 3%.

IN-AIR DETECTOR

Inspired by efforts at ESRF to use unwanted very hard x-rays penetrating the accelerator vacuum chamber as a high-resolution beam size / position diagnostic, and considering also that an in-air vibrating wire monitor is expected to have a response time well below 1 second, a five-wire unit was designed and built at the Yerevan Physics Institute. This detector was designed to include five horizontally-mounted 100-micron-diameter steel wires with approximately 0.5-mm separation between them, to be mounted at an unused bending magnet radiation port in APS sector 37. Also included in the design was the ability to rotate the plane of the wires about a horizontal axis so as to reduce the effective vertical wire separation. The detector is shown in Figs. 4 and 5.

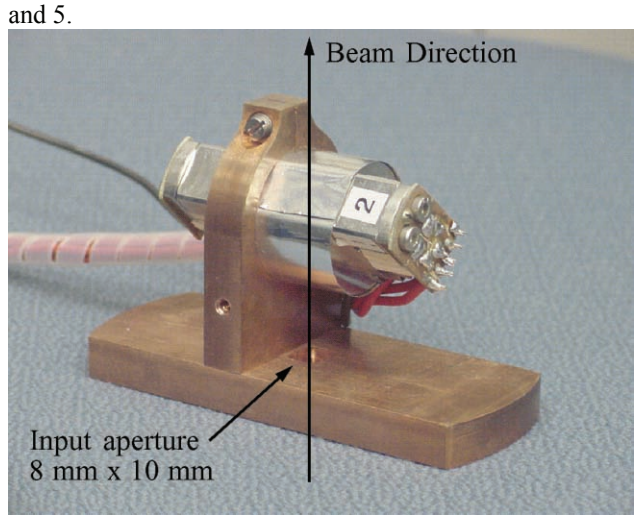

Figure 4: Five-wire in-air VWM unit showing rotational degree of freedom.

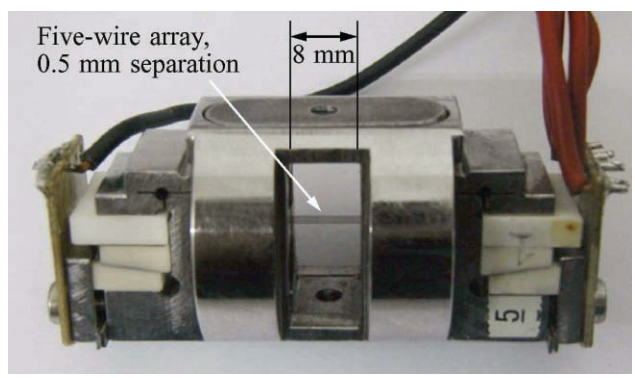

Figure 5: Five-wire VWM detector detail.

The wires themselves are 36 mm long and made of thermally-treated stainless steel [10]. The horizontal aperture of the detector is 8 mm, with a variable vertical aperture depending on the rotation angle. Acoustic resonance frequencies fall in the range from 4000 to 9000 Hz, with 0-1000 Hz variability from induced thermal heating allowed. The thermal calibration factor is nominally 40 Hz / K at 4200 Hz operating frequency. This results in a wire temperature range of 0 to 25 K, resolution of 0.00025 K, and long-term stability rated at +/- 0.00025 K and +/- 0.001 K over 1- and 24-hour periods, respectively.

The device shown in Fig. 4 (actually a second unit nearly identical to it) was installed at an unused bending magnet beamline exit port flange in sector 37. This sector is reserved for rf cavities, and as such no beamline will ever be constructed there. Shown in Figs. 6 and 7 are a photo of the photon beam dump absorber together with a line drawing, and a rendering of the installed detector.

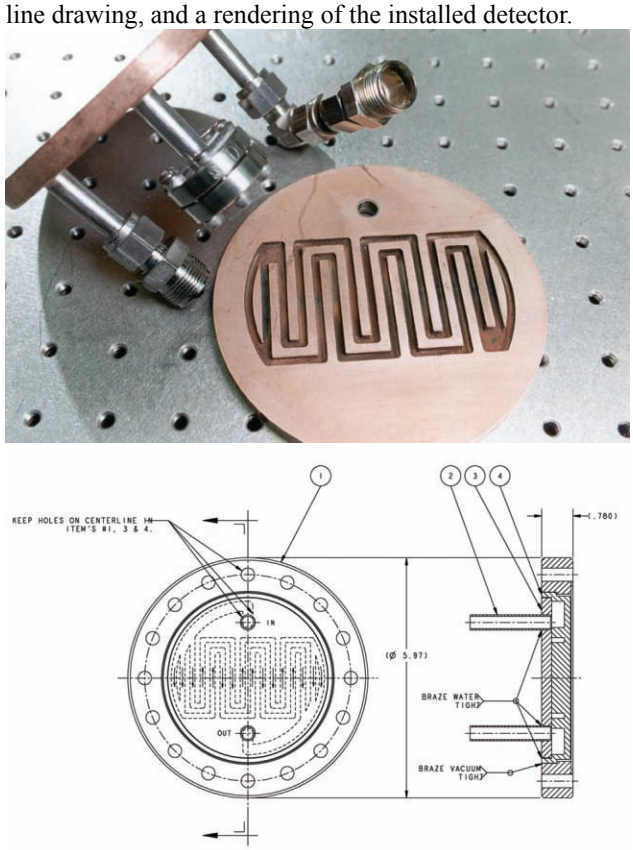

Figure 6: Bending magnet photon beam dump for unused exit port locations. Top: Disassembled unit showing internal cooling channels. Bottom: Assembly drawing.

The actual installation was significantly less tidy than shown in Fig. 7, but due to constraints of schedule pressure it was sufficient to produce acceptable results. The flange assembly is mounted 6.4 meters downstream of the bending magnet source point. At the APS, the source point is defined to be one-eighth of the way into the dipole magnet steel starting from the upstream end. A tangent line attached to the nominal curved particle beam trajectory at the one-eighth point in principle should strike the center of this flange. The flange thickness is 20 mm, which is the same as the copper thickness with the exception of the cooling channels. The flange diameter is 6 inches. A few variations of this design exist, as can be seen from the photo in Fig. 6 vs. the line drawing, which is what is actually installed in sector 37.

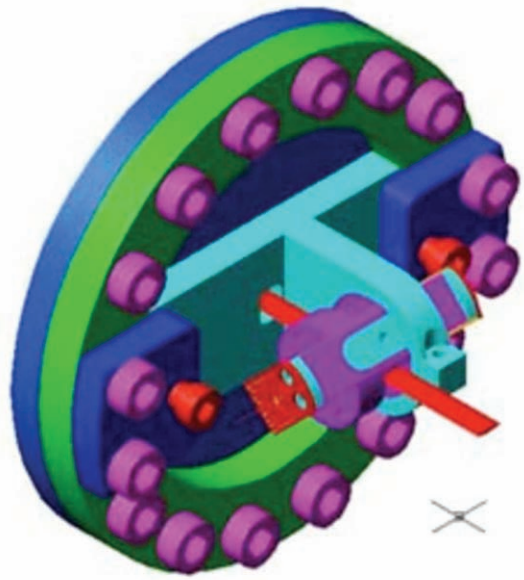

Figure 7: Conceptual rendering of the VWM installation.

DATA COLLECTION

After storing 102 mA in the APS storage ring, distributed among 324 individual bunches for long lifetime, a special vertical orbit bump was created to allow angle steering at the 37-BM bending magnet source point. An initial large-range scan had produced a measurable blip at an angle of -0.5 mrad relative to the nominal stored beam trajectory. This was due to a rather hasty installation effort that placed the detector's active area 3 mm below the machine midplane. After a second preliminary scan to define the optimal scan range, a series of scans over a 250 microradian range with 125 steps of 2 microradians each was collected. Typical results for one of these scans is shown in Fig. 8. While the orbit was scanned with 125 steps, VWM data was collected at a constant 1 Hz throughout.

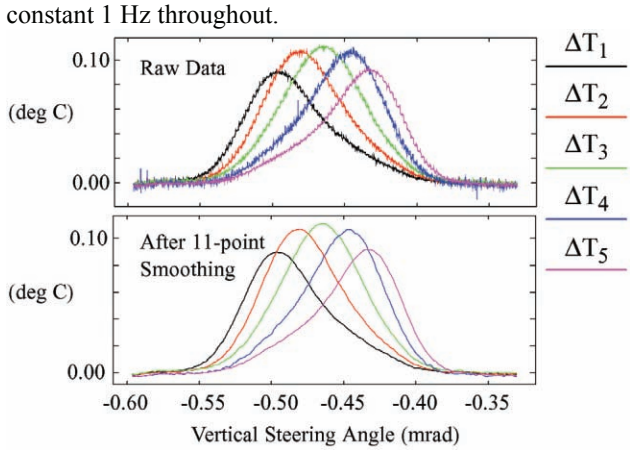

Figure 8: VWM-005 results from a vertical angle scan at source point 37-BM.

The horizontal axis is computed from rf BPMs straddling the source point, after correcting for a bunch-pattern-dependent change in gain. The dominant mode of operation at APS uses 24 bunches, but for 324-bunch operation, the rf BPM calibrations can change by 15% or more. Using 324 bunches has the side benefit of providing a longer beam lifetime. The lower panel of Fig. 8 shows the same data after running it through an 11-point smoothing filter with a despiking algorithm to eliminate outliers [11].

Immediately it is apparent that the in-air detector produces a different profile depending upon which wire is chosen. This is actually a cross-talk phenomenon where convective heat transfer is occurring between the wires, in spite of the fact that their temperatures differ by only small fractions of a degree. Using a linear heat-transfer model described in reference [8], the relative power striking each wire can be inferred from a matrix connecting the temperature differences between wires. This matrix is constructed semi-empirically, from the requirement that all wires produce the same power profile. The matrix used for the analysis presented here is contained in Table 1.

Table 1: Linear Heat Transfer Coupling Matrix

α_{ij}	ΔT_1	ΔT_2	ΔT_3	ΔT_4	ΔT_5
ΔT_1	2.50	0.633	0.353	0.319	0.170
ΔT_2	0.633	1.865	0.882	0.434	0.183
ΔT_3	0.353	0.882	1.692	0.932	0.424
ΔT_4	0.319	0.434	.932	1.820	0.489
ΔT_5	.170	.183	.424	.489	2.478

Starting from the smoothed data in Fig. 8, application of the heat transfer matrix results in the power profiles shown in Fig. 9, together with corresponding Gaussian fits. The data of Fig. 8 was first normalized to compensate for the slight decay in stored beam current over the course of the scan.

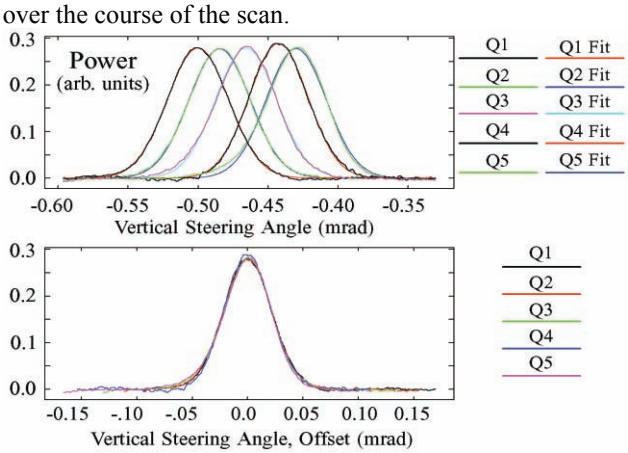

Figure 9: APS bending magnet power density profiles inferred from VWM data. Top: Measured profiles together with Gaussian fits. Bottom: The same measured data, shifted along the horizontal axis.

The upper panel in Fig. 9 shows the result of applying the coupling matrix to the smoothed data of Fig. 8, but with the additional step of subtracting a baseline power level for each curve, which is derived from the individual Gaussian fits. In the lower panel a similar offset has been introduced along the horizontal axis for direct comparison of the profiles from each wire. Only the data is shown in the lower panel, with no fit data displayed.

Shown in Table 2 are the Gaussian fit parameters for the curves of Fig. 9.

Table 2: Profile Fit Parameters

	gfit Centroid		gfit Sigma	
	mrad	mm	microrad	microns
ΔT_1	-0.5001	-3.201	21.96	140.5
ΔT_2	-0.4847	-3.102	21.95	140.5
ΔT_3	-0.4657	-2.981	21.87	140.0
ΔT_4	-0.4426	-2.833	21.01	134.5
ΔT_5	-0.4300	-2.752	21.51	137.7

The columns listed in mm / microns were derived from the angular data via multiplication by the 6.4-meter source-detector distance. Note that the sigma value for wire 4 deviates significantly from the values for the other wires. As can be seen from the original data, as well as in the lower panel of Fig. 9, this wire was producing data that was generally noisier than that of the other wires. A second observation is that difference between centroid values of wires 1 and 5 indicate an overall vertical extent of only 449 microns. Keeping in mind that the nominal separation between individual wires is 500 microns, this implies that the plane containing the wire is inclined at a shallow angle relative to the horizontal. Specifically, one expects an inclination angle of atan(0.449 / 2) = 12.65 degrees. This was cause for a bit of consternation since the spare unit had an angle nearer to 45 degrees. However, an inspection of the in-tunnel unit during a later maintenance period confirmed the shallow angle.

The values of rms beam size (gfit Sigma) in the table are certainly of the correct order of magnitude. An old calculation done by Ken Green many years ago showed that a Gausian fit to the power density for a bending magnet radiation source is fit quite well if one uses an rms angular size of 0.608 / γ, where γ is the relativistic factor, equal to 13700 for the 7-GeV APS [12]. This yields an rms size of 44 microradians. As shown in Fig. 10, however, the hard x-rays capable of penetrating 20 mm of copper have a considerably smaller profile than those at the critical energy. This is a plot of radiated power per unit solid angle for circular motion into revolution harmonic n as a function of vertical angle ψ. This is from a calculation done in 1945 by Schwinger [13,14]. In this case, the classical definition of the critical photon energy, which is 19.5 keV for APS bend magnets, corresponds to n = 3/2. The highest energy curve shown, curve J, corresponds to a photon energy of just under 100 keV. Unfortunately, in order to calculate the curves of Fig. 10, one is required to compute Bessel function of order n with arguments also of order n, where n is of order γ^3 = 3e12.

The data for Figs. 8 and 9 were collected with horizontal / vertical machine coupling set at 5.3%, corresponding to a vertical emittance of 0.15 nm-rad, a

vertical particle beam source size of 58 microns rms, and angular divergence of 3 microradians rms. This is quite a large amount of coupling, since the APS is normally run with 1% coupling, and was done intentionally using a skew quadrupole magnet to investigate whether the VWM could detect changes in vertical beam size. During an earlier scan, the coupling was set at an average 2.6% corresponding to a source size of 40 microns rms and angular divergence of 2 microradians rms. Because the initial steering angle was so large (-0.5 mrad), the coupling was influenced by forcing the trajectory to be so far off axis through a large number of sextupole magnets. This also caused the coupling to change significantly over the course of a single scan, from 3.6% at the extreme limit of the scan to 1.7% at the other end. Shown in Table 3 are the results of this earlier scan.

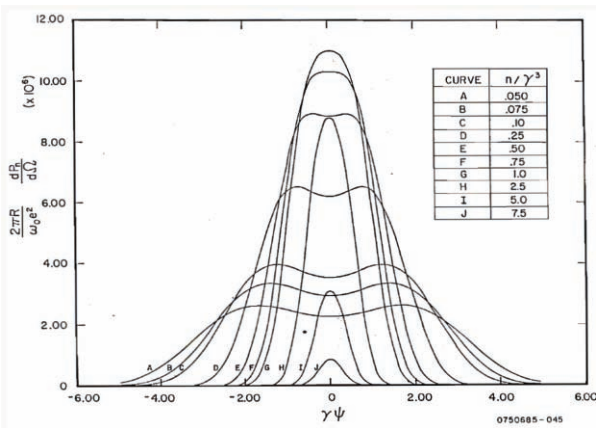

Figure 10: Synchrotron radiation power per unit solid angle into revolution harmonic n as a function of vertical angle ψ. The quantity γ is the relativistic factor.

Table 3: Fit Parameters for 2.6% Average Coupling

	gfit Centroid		gfit Sigma	
	mrad	mm	microrad	microns
ΔT_1	-0.4924	-3.151	19.88	127.2
ΔT_2	-0.4768	-3.052	19.96	127.7
ΔT_3	-0.4577	-2.930	20.00	128.0
ΔT_4	-0.4352	-2.785	19.29	123.4
ΔT_5	-0.4221	-2.701	19.43	124.3

From the table, it is clear that the effects of the coupling change are resolved by this detector. Due to the complex nature of off-axis trajectories through sextupoles it is difficult to make any quantitative statements; however, the observed resolution is very encouraging. Note that the measured distance between centroids for wires 1 and 5 is now 450 microns to be compared with 449 microns for Table 2.

CONCLUSIONS

Vibrating wire monitors have proven themselves as a reliable quantitative diagnostic of beam size and position for hard x-ray synchrotron radiation. For the five-wire design, using a shallow inclination angle allowed for an effective vertical wire separation distance of only 112 microns. Because of this, a five-sample beam profile monitoring vertical beam sizes with sigma values as small as 100 microns rms or lower can be provided in real time. As at ESRF, widespread use of monitors of this type could allow for local coupling correction around the ring. Further potential uses are envisioned, such as integrating an in-air monitor into an undulator photon mask assembly for clean hard x-ray position measurements.

REFERENCES

[1] G. Decker, O. Singh, Phys. Rev. ST Accel. Beams 2, 112801 (1999).
[2] R. Alkire, G. Rosenbaum, and G. Evans, J. Synchrotron Rad. 7, 61-68 (2000).
[3] G. Decker, G. Rosenbaum, and O. Singh, "Development of a Hard X-ray Beam Position Monitor for Insertion Device Beams at the APS," BIW '06, Batavia, IL, AIP Conf. Proc. 868, 202-207 (2006).
[4] G. Decker, P. Den Hartog, O. Singh, G. Rosenbaum, "Progress Toward a Hard X-ray Insertion Device Beam Position Monitor at the Advanced Photon Source," PAC '07, Albuquerque, May 2007, p. 4342.
[5] S.G. Arutunian et al., "PETRA Proton Beam Profiling by Vibrating Wire Scanner," DIPAC '05, Lyon, June 2005, p. 181.
[6] B.K. Scheidt, "Detection of Hard Xrays in Air for Precise Monitoring of Vertical Position and Emittance in the ESRF Dipoles," DIPAC '05, Lyon, June 2005, p. 238.
[7] G. Decker, S.G. Arutunian, M. Mailian, G. Rosenbaum, "First Vibrating Wire Monitor Measurements of a Hard X-ray Undulator Beam at the Advanced Photon Source," DIPAC '07, Venice Maestra, May 2007, to be published.
[8] S.G. Arutunian, "Vibrating Wire Sensors for Beam Instrumentation," these proceedings.
[9] R. Dejus, private communication, Argonne National Laboratory.
[10] Vibrating wire monitor VMW-005 users manual, HTM Reetz GmbH, Berlin, Germany, in cooperation with Yerevan Physics Institute.
[11] M. Borland, L. Emery, H. Shang, R. Soliday, "User's Guide for SDDS Toolkit Version 1.30," http://www.aps.anl.gov/Accelerator_Systems_Division/Operations_Analysis/manuals/SDDStoolkit/SDDStoolkit.html
[12] G.K. Green, "Spectra and Optics of Synchrotron Radiation," BNL report 50522.
[13] J. Schwinger, "On Radiation by Electrons in a Betatron," Office of Naval Research (1945), transcribed by M. Furman as Lawrence Berkeley National Lab note LBNL-39088 (1999).
[14] J. Schwinger, Phys. Rev. 70, 798 (1946).